

First Principles Investigation of the Influence of Varied Cr Atom on Band Structure and Magnetic Moment of Rutile SnO₂

Funmilayo Ayedun, Etido P. Inyang and Efiang A. Ibanga

Received 18 November 2020/Accepted 24 December 2020/Published online: 30 December 2020

Abstract: *The electronic and magnetic properties of SnO₂ doped with various compositions of chromium atoms are reported. Studies on magnetic property of Cr_xSn_{1-x}O₂ compounds features possible room temperature ferromagnetism which increased nonlinearly as Sn atom is replaced with Cr atom, at $x = 0.25$ (1.9976 μ B), $x = 0.50$ (3.9309 μ B), $x = 0.75$ (5.8831 μ B) and $x = 1.00$ (7.821 μ B). The magnetic moment and bandgap energy of undiluted SnO₂ were compared at $x = 0$. The addition of Cr atom into SnO₂ enhanced the shift from pure binary nonmetallic system to ternary metallic compound. The direct energy gaps decrease from $x = 0$ to 0.5, and increase from $x = 0.75$ to 1.00.*

Keywords: Rutile, First-principles, Generalized Gradient Approximation (GGA), Magnetic moment, magnetic dipole moment.

F. Ayedun

Department of Pure and Applied Science, National Open University of Nigeria, Abuja, FCT, Nigeria

Email: fayedun@noun.edu.ng,

funmiayedun@yahoo.com

Orcid id: 0000-0001-5421-9305

Etido P. Inyang

Department of Pure and Applied Science, National Open University of Nigeria, Abuja, FCT, Nigeria

Email: etidophysics@gmail.com

Orcid id: 0000-0002-5031-3297

E.A. Ibanga

Department of Pure and Applied Science, National Open University of Nigeria, Abuja, FCT, Nigeria

Email: eibanga@noun.edu.ng

Orcid id: 0000-0002-5452-0613

1.0 Introduction

Dilute magnetic semiconductors doped with transition metals are currently receiving research interest because of their functionalities in the production of spin transistors as well as light-emitting diodes (Ogale, 2010). Stannic oxide

(SnO₂) is a wide-band n-type semiconductor material and it has application potential in photo decadence of organic substances, catalysts, coatings, optoelectronic devices and resistors, opacifiers, photosynthesis, etc.

Electrons in an atom perform orbital and spin motions which are capable of producing a magnetic field. Strong or weak magnetism in materials; is a function of magnetic moments produced from the amperian currents and can be segmented into: ferromagnetism, diamagnetism, paramagnetism, antiferromagnetism and ferrimagnetism (Okeke *et al.*, 2000). Ferromagnetic materials exist in domains with varying magnetic moments. In the presence of an externally applied magnetic field, the aligned magnetic moments within domains become magnetized with a very strong internal magnetic field (Okeke *et al.*, 2000).

Ferromagnetism tends to diminish with an increase in temperature but gradually vanishes as the Curie temperature is reached. A Ferromagnetic material comprises of soft materials, hard materials and ferrites and they have permeability greater than one. These materials are useful in the production of permanent magnets, transformer core, magnetic tapes and memory storage devices and some components in the automobile, electronic sector, communication and aviation industries. They are also useful in realizing magnetic resonance imaging and magnetic screening.

Ternary and quarternary diluted magnetic semiconductor materials are transition metal-doped systems that reveal the room temperature ferromagnetism (Fukumura *et al.*, 2005). Some studies have been reported on first principles electronic calculations concerning rutile SnO₂. For example, Borges *et al.* (2011) carried out such calculations within the spin density functional theory, alternated magnetic and nonmagnetic layers of rutile-CrO₂ and rutile SnO₂. They observed a half-filled for the (CrO₂)_n(SnO₂)_nSL_s at all values of n. The ground state was found to be Ferromagnetic (FM) with a magnetic moment of 2

μ B. Abdulsattar *et al.*(2016) reported effects of Indium doped tin oxide by both experimental and theoretical approaches. Their experimental results through XRD, UV-Vis and Raman spectroscopy reveal that as lattice constants increased, there was a decrease in energy gap. The DFT method via Large unit cell showed a change in experimental stoichiometry as the lattice constant before and after the doping are almost the same.

In view of the significant of the magnetic and electronic structure of rutile SnO₂ on the potential applications of previous works, the present study is aimed at investigating the influence of varied Cr atom on band structure and magnetic moment of rutile SnO₂

2. 0 Computational Details

All computational calculations were performed using the Perdew- Burke – Ernzhof - Projected Augmented Wave (PBE-PAW) pseudopotentials from the Quantum espresso library (Gianozzi *et al.*, 2009). A six atom supercell was built for an undiluted binary SnO₂ at x = 0. Twelve atoms supercell comprising of four atoms of tin and eight atoms of oxygen were employed at x = 0.25 to 1 with Cr atom replacing Sn atom at x = 0.25 to 1. A Monkhorst- Pack k-point of 10x10x5 was applied for SnO₂ at x = 0, with an energy, cut-off of 80 Ry. At x = 0.25 to 1, for a twelve atom supercell used, the k-points were set at 10x10x5, 8x8x4, 10x10x5 and 10x10x5 with an energy cut off of 90Ry.

2.1 Methodology

The magnetic moment (m) depicts the magnetic strength and magnetic orientation which brings about a magnetic field. It aligns with an external applied magnetic field and links torque (τ) of an object such as permanent magnets, astronomical objects, elementary particles and loops of electric current to the magnetic field (B). This can be expressed mathematically as:

$$\tau = m \times B \quad (1)$$

The magnetic field of a magnetic dipole is proportional to its magnetic dipole moment (μ). The magnetic dipole is a measure of a dipole's ability to turn itself into alignment with a given external magnetic field. The magnitude of energy (E) of magnetic dipole moment (μ) is a function of the alignment of magnetic field (B). That is,

$$E = - \mu \times B \quad (2)$$

Electrons possess inherent magnetic moments which are related to their spin angular momentum. In the presence of a magnetic field, an electron has one of two orientations in agreement with the magnetic spin quantum number. And the spin polarization is the ratio of the density of states up-spin to down spin electrons at a Fermi level (Yasuhiko *et al.*, 2011). The polarization of the electronic spins leads to magnetization density because magnetization is a function of the ground state charge density and any other ground state property. The magnetic dipole moment per unit volume is:

$$M (r) = \sum_i N_i \langle m_i \rangle \quad (3)$$

where $\langle m_i \rangle$, the average magnetic dipole moment of the i^{th} is the type of molecule in the vicinity of point r and N_i is the number of such molecules per unit volume at r.

The energy gap between the uppermost valence band and the minimum conduction band differs for various materials. It decides the electrical conductivity and electronic transport of a solid, and classifies materials into insulators, semiconductors and conductors. Energy gaps due to varying concentrations of chromium atom into SnO₂ were examined using a modified form of Vegard's law (Ayedun *et al.*, 2017):

$$E_g(A_x B_{1-x} C) = xE_{AC} + (1-x)E_{BC} - x(1-x)b_E \quad (4)$$

3.0 Results and Discussion

3.1 Band structural property

The band structures along the high symmetry paths were observed in this study at x = 0, 0.25, 0.50, 0.75 and 1.00 as shown in Figs. 1 to 5 respectively. A bulk binary SnO₂ at x = 0 is characterized with a direct bandgap; which is feasible at Γ to Γ with direct energy of 1.163eV. The energy gap obtained is closer to the energy gap of 1.25eV reported by Deligoz *et al.* (Deligoz, 2007). Also, indirect energy gaps were achieved from M to Γ at x = 0.25, Z to Γ at x = 0.75 and Γ to X at x = 1.00 respectively while the direct energy gap was attained from Γ to Γ at x = 0.5. The energy gaps varied nonlinearly as the dopant, Cr atom increased.



The energy gaps were computed using equation (4). The most stable phase of the material, $\text{Cr}_x\text{Sn}_{1-x}\text{O}_2$ is at $x = 0.25$ with the bowing energy parameter of 0.385eV. This will be of immense value in the production of spintronic devices and spin-polarized light-emitting diodes. There is a hybridization between O-2p state at the topmost valence band of SnO_2 and minimum conduction, Sn-5p state at $x = 0$. For the compositions $x = 0.25$

to 0.75, the uppermost valence band was observed at O-2p state while the conduction bands were predominated by Sn-5p state and Cr- 3d state. At $x = 1$, the lowest conduction band was dominated by Cr- 3d state and the topmost valence band by O-2p state. The values of band energies of $\text{Cr}_x\text{Sn}_{1-x}\text{O}_2$ obtained in this study are reported in Table 1.

Table 1: Energy gaps of $\text{Cr}_x\text{Sn}_{1-x}\text{O}_2$ materials

| Compositions (x) | System | Present Study (eV) | Experimental(eV) | Theoretical |
|------------------|--|--------------------|------------------|-----------------|
| 0.00 | SnO_2 | 1.163 | 3.61[4] | 1.25 [15] |
| 0.25 | $\text{Cr}_{0.25}\text{Sn}_{0.75}\text{O}_2$ | 1.000 | | |
| 0.50 | $\text{Cr}_{0.50}\text{Sn}_{0.50}\text{O}_2$ | 0.389 | | |
| 0.75 | $\text{Cr}_{0.75}\text{Sn}_{0.25}\text{O}_2$ | 0.634 | | |
| 1.00 | CrO_2 | 0.800 | 0.00 | 1.34[5], .5[16] |

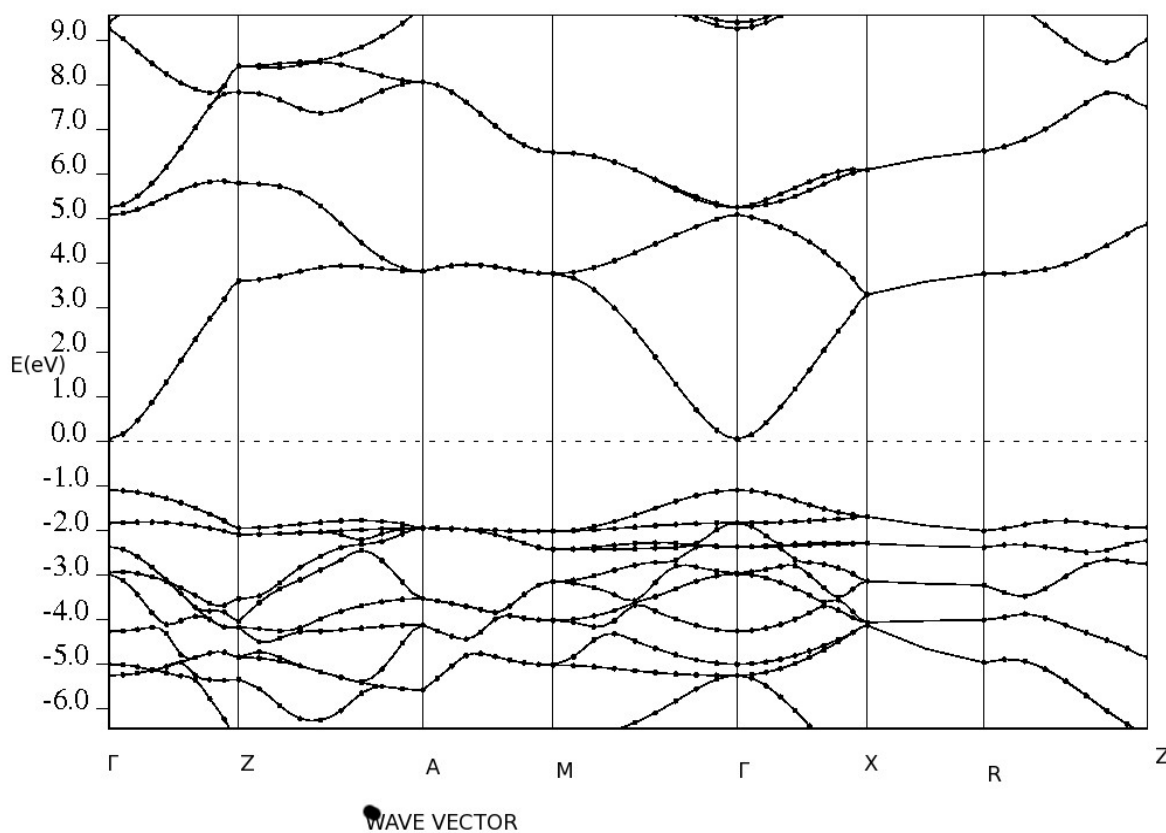


Fig. 1: Band structure of SnO_2 .



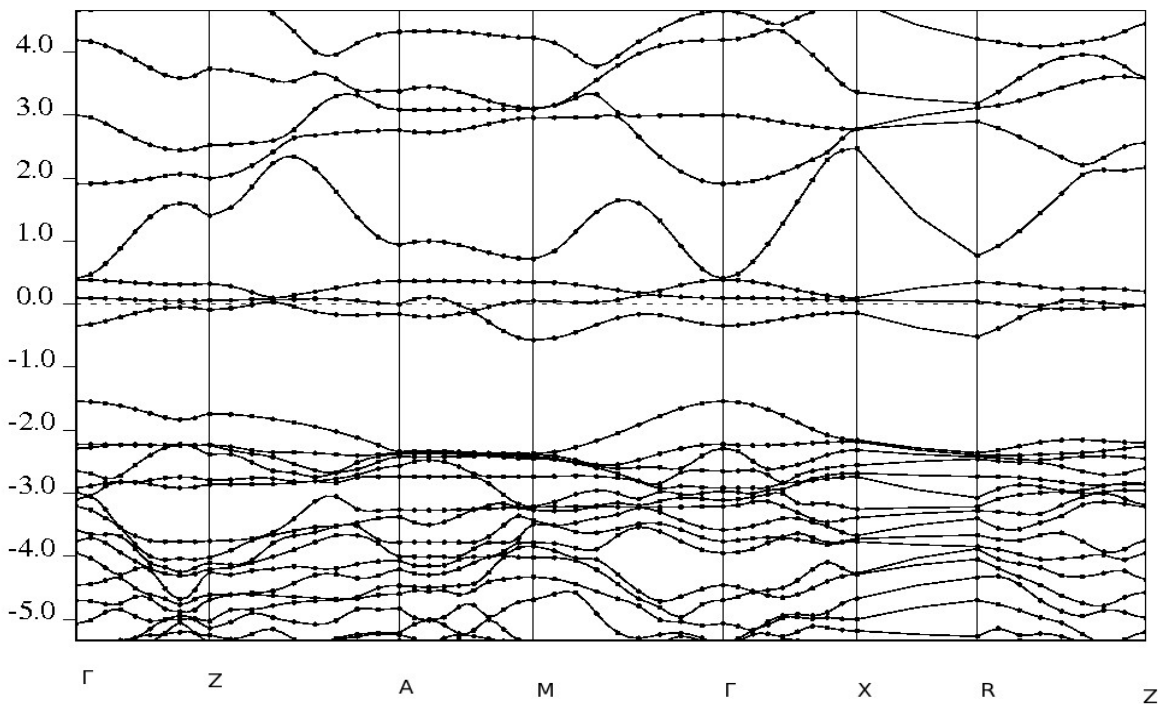


Fig. 2: Band structure of $\text{Cr}_{0.25}\text{Sn}_{0.75}\text{O}_2$.

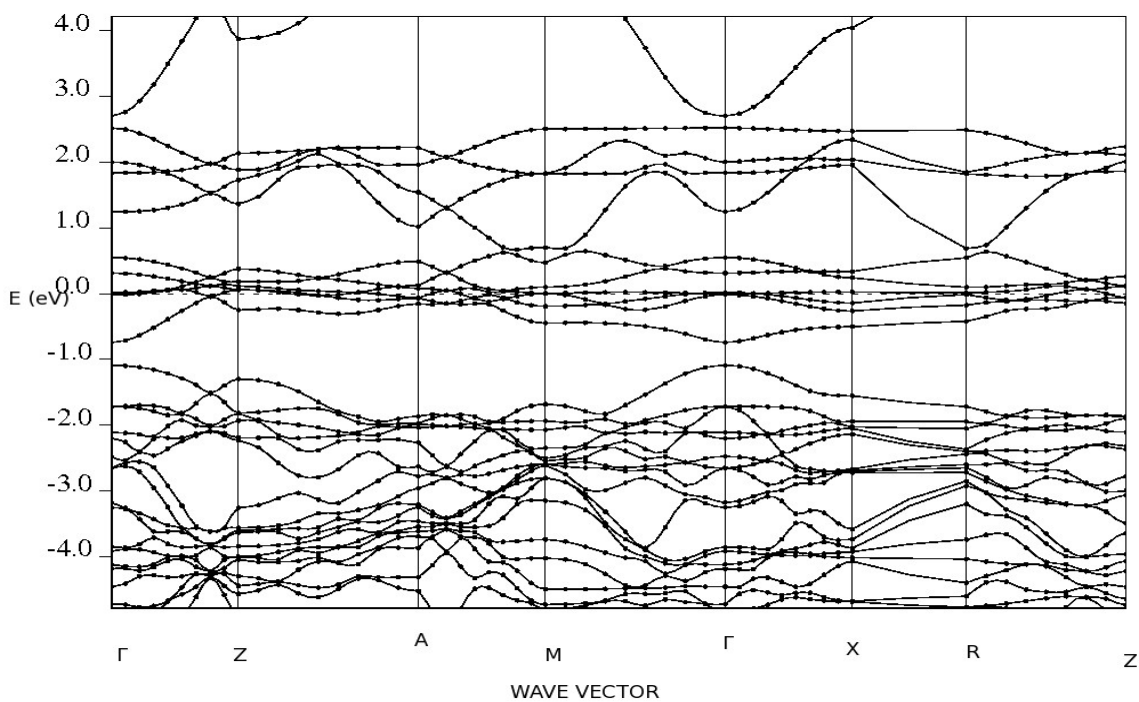


Fig. 3: Band structure of $\text{Cr}_{0.50}\text{Sn}_{0.50}\text{O}_2$.



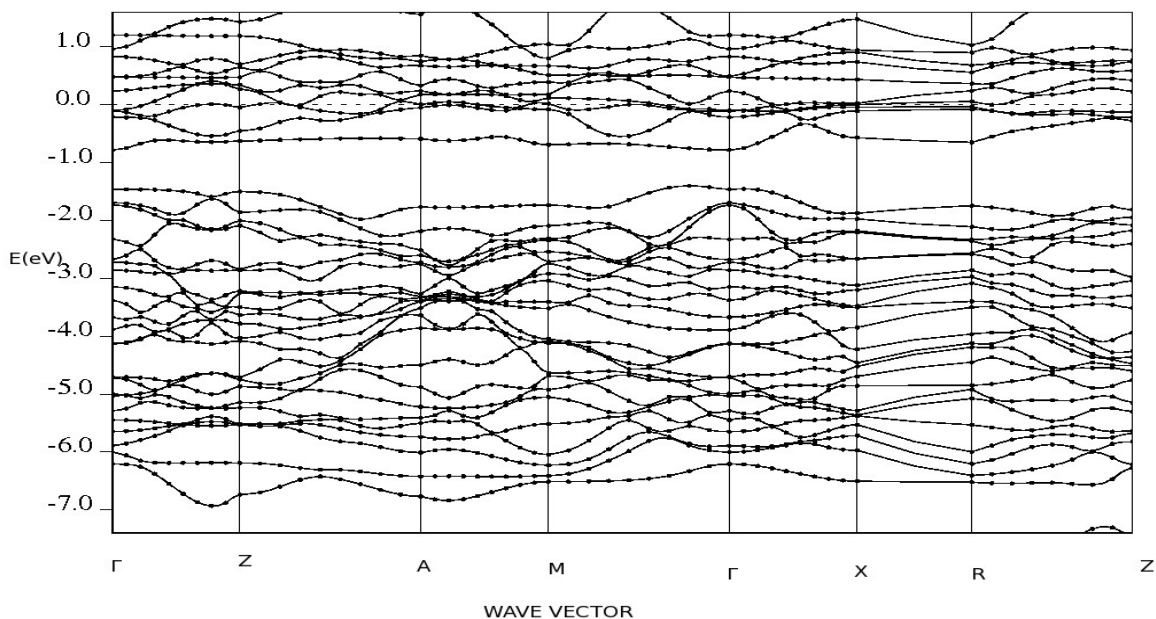


Fig. 4: Band structure of Cr_{0.75}Sn_{0.25}O₂.

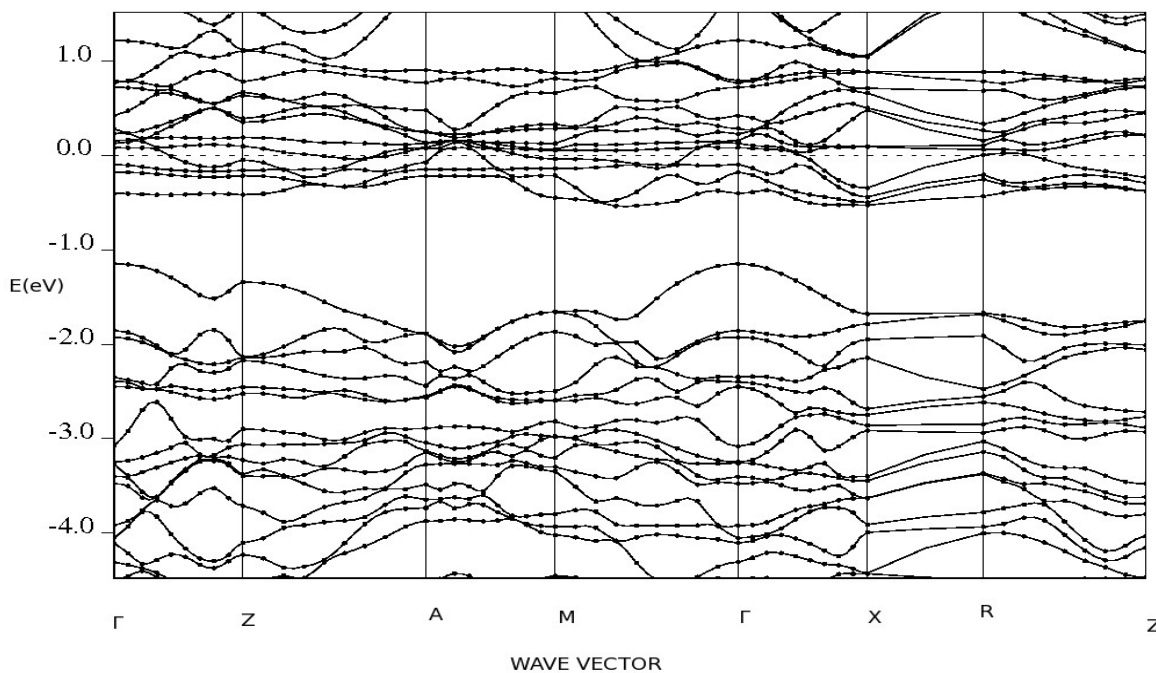


Fig. 5: Band structure of CrO₂.

3.2 Magnetic Property

The magnetic moment of paired Sn²⁺ and O²⁻ in pure SnO₂ was found to be zero, which is in agreement with the observations made by Wang (2010), Gu *et al.* (2008). SnO₂ doped with Cr atom exhibited a shift in transition from nonmetal to

ferromagnetic materials at x = 0.25 to 1. The resultant magnetic moment increased nonlinearly with a rise in composition of Cr atom and their unpaired valence electrons were: Sn (4d¹⁰5s²5p²), Cr (3s²3p⁶3d⁴) and O (2s²2p⁴).



The bar chart in Fig. 6 depict the nonlinear increase in the magnetic moment of $\text{Cr}_x\text{Sn}_{1-x}\text{O}_2$ materials with varied Cr atom while detailed magnetic moments of the system under study is presented in Table 2.

Table 2: Magnetic moment of $\text{Cr}_x\text{Sn}_{1-x}\text{O}_2$ materials

| Compositions (x) | System | Present Study(μB) | Experimental | Theoretical |
|------------------|--|--------------------------------|--------------|-------------|
| 0.00 | SnO_2 | 0 | 0 [19] | 0 [11] |
| 0.25 | $\text{Cr}_{0.25}\text{Sn}_{0.75}\text{O}_2$ | 1.9976 | | |
| 0.50 | $\text{Cr}_{0.50}\text{Sn}_{0.50}\text{O}_2$ | 3.9309 | | |
| 0.75 | $\text{Cr}_{0.75}\text{Sn}_{0.25}\text{O}_2$ | 5.8831 | | |
| 1.00 | CrO_2 | 7.8271 | | 9.0 [9] |

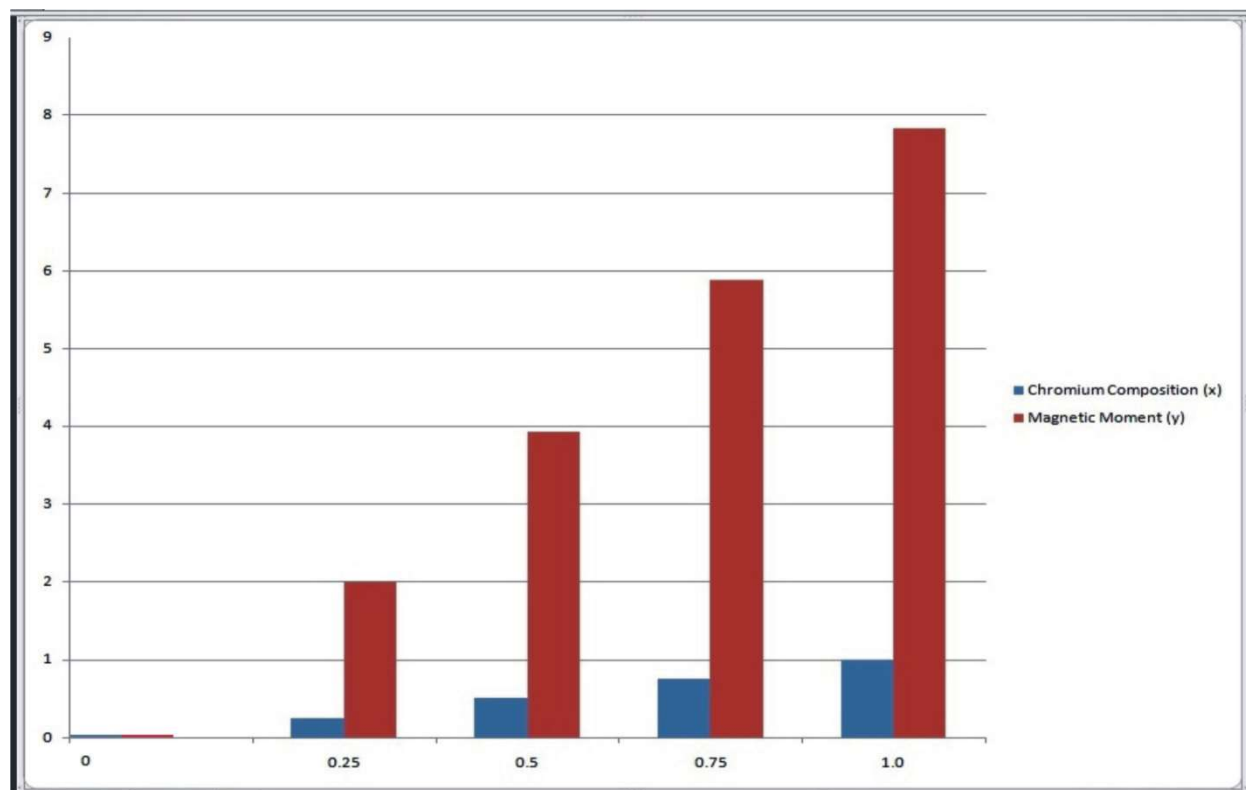


Fig. 6: Complex bar chat of magnetic moment of $\text{Cr}_x\text{Sn}_{1-x}\text{O}_2$ compound.

4.0 Conclusion

Self-consistent PBE-PAW calculations using GGA approach between exchange correlations based on density functional theory were carried out on $\text{Cr}_x\text{Sn}_{1-x}\text{O}_2$ materials. The results obtained indicated that the showed excellent agreement between the experimental and theoretical magnetic moment of pure SnO_2 . The most stable phase of these materials was revealed at $x = 0.25$. The energy gap is in close agreement with theoretical data and 0.67 per cent error with that of experimental.

5.0 References

- Abdulsattar, M. A, Batros, S. S. & Addie, A. J. (2016). Indium doped SnO_2 nanostructures preparation and properties supported by DFT study. *Superlattices and Microstructures* 100, 342-349.
<https://doi.org/10.1016/j.spmi.2016.09.042>
- Allegre, V., Mainault, A., Lehmann, F., Lopes, F. & Zamora, M. (2014). Self-potential response to drainage-imbibition cycles. *Geophysical*



- Journal International*, 197,3, pp. 1410-424. <https://doi.org/10.1093/gji/-ggu055>.
- Ayedun, F., Adebambo, P. O., Adetunji, B. I., Ozebo, V. C., Oguntuase, J. A. & Adebayo, G. A. (2017). Increased Malleability in tetragonal $Zr_xTi_{1-x}O_2$ Ternary Alloys: First-Principles Approach. *De Gruyter. Z. Naturforsch.* 2017; aop<https://doi.org/10.1515/zna-2017-0036>.
- Beltran, A., Andres, J., Sambrano, J. R. & Longo, E. (2008). Density Functional theory on the structural and electronic properties of low index rutile surfaces for $TiO_2/SnO_2/TiO_2$ and $SnO_2/TiO_2/SnO_2$ composite systems. *Journal of Physical Chemistry A.*, 112, pp. 8943-8952
- Brener, N. E., Tyler, J. M., Callaway, J., Bagayoko, D. & Zhao, G. L. (2000). *Physical Review B*. 61, 24 DOI:<https://doi.org/10.1103/PhysRevB.61.16582>.
- Borges, P.D., Scolfaro, L.M., Leite Alves, H. W., Silva Jr, F. F. & Assali, L. V. C. (2011). Electronic and magnetic properties of SnO_2/CrO_2 thin superlattices. *Nanoscale Research Letters*, 6, 146, <https://doi.org/10.1186/1556-276X-6-146>
- Deligoz, E., Colakoglu, K. & Cifti, Y. O. (2007). The structural, elastic and electronic properties of the pyrite-type phase of SnO_2 . *Journal of Physics and Chemistry of Solids*, 69, 4, pp. 859-864.
- Fukumura, T., Toyosaki, H. & Yamada, Y. (2005). Magnetic oxide semiconductors. *Semiconductor Science and Technology*, 20, 4, pp. S103- S111.
- Jeng, H. & Guo, G. Y. (2002). First-principle investigations of the orbital magnetic moments in CrO_2 . *Journal of Applied Physics*, 92, 2, pp. 951-957, <https://doi.org/10.1063/1.1486260>
- Gianozzi, P., Baroni, S., Bonini, N., Calandra, M., Car, R., Cavazzoni, C., Ceresoli, D., Chiarotti, G. L., Cococcioni, M., Dabo, I., Dal Corso, A., de Gironcoli, S., Fabris, S. Fratesi, G., Gebauer, R., Gerstmann, U., Gougoussis, C., Kokalj, A., Lazzeri, M., Martin-Samos, I., Marzari, N., Mauri, F., Mazzarello, R., Paolini, S., Pasaquarello, A., Paulatto, L. Sbraccia, C., Scandolo, S., Sclauzero, G., Seisonen, A. P. Smogunov, A., Umari, P. & Wentzcovitch, R. M. (2009). *Journal of Physics: Condensed Matter*. 395502 <https://iopscience.iop.org/journal/0953-8984>
- Gul, R. Victor, M. G. & Soon, C. H. (2012). Vacancy-induced magnetism in SnO_2 . A density functional study. *Physical Review B* 78, 184404-184408. DOI: <https://doi.org/10.1103/PhysRevB.78.184404>
- Monkhorst, H. J. & Park, D. (1976). Special points for Brillouin-zone integrations. *Physical Review B* 13, 5188-5192. <http://dx.doi.org/10.1103/PhysRevB.13.5188>
- Ogale, S. (2010). Dilute doping, defects and ferromagnetism in metal oxide systems. *Advanced Materials*, 22(29) 312.
- Okeke, C. E., Okeke, P.N., Ofoegbu, C. O. & Ubachukwu, A. A. , Unaogu, L. A. (2000) *Electromagnetism and /modern Physics for Life Sciences*. ISBN: 9782461423
- Stashans, A., Puchaicela, P. & Rivera, R. (2014). DFT study of Chromim-doped SnO_2 materials. *Journal of Material Science*, 49, pp. 2904-2911. ISSN 0022-2461, DOI 10.1007/s10853-013-7999-9.
- Schlottmann, P. (2003). Double exchange mechanism for CrO_2 . *Physical Review B* 67, 174419. DOI:<https://doi.org/10.1103/PhysRevB.67.174419>
- Vidhu, V. K. & Philip, D. (2015). Photosynthesis and applications of bioactive SnO_2 nanoparticles. *Materials Characterization*, 101, pp. 97-105. <https://doi.org/10.1016/j.matchar.2014.12.027>
- Yasuhiko, T. Yoji, I. & Toshiya, K. (2011). Spin-polarized electronic band structures of the Fe_4N-Co_4N system. *Journal of Magnetism and Magnetic Material*, 323, 23, pp. 2941-2944.
- Wang, C., Ge, M. & Jiang, J. Z. (2010). Magnetic behavior of SnO_2 nanosheets at room temperature. *Applied Physics Letters* 97, pp. 042510 – 042513.

Conflict of interest

The authors declared no conflict of interest

